ORIGINAL RESEARCH

Increased Stiffness Is the Major Early Abnormality in a Pig Model of Severe Aortic Stenosis and Predisposes to Congestive Heart Failure in the Absence of Systolic Dysfunction

Kiyotake Ishikawa, MD; Jaume Aguero, MD; Jae Gyun Oh, PhD; Nadjib Hammoudi, MD; Lauren A. Fish; Lauren Leonardson, LVT; Belén Picatoste, PhD; Carlos G. Santos-Gallego, MD; Kenneth M. Fish, PhD; Roger J. Hajjar, MD

***Background*—**It remains unclear whether abnormal systolic function and relaxation are essential for developing heart failure in pathophysiology of severe aortic stenosis.

***Methods and Results*—**Yorkshire pigs underwent surgical banding of the ascending aorta. The animals were followed for up to 5 months after surgery, and cardiac function was assessed comprehensively by invasive pressure–volume measurements, 3-dimensional echocardiography, echocardiographic speckle-tracking strain, and postmortem molecular and histological analyses. Pigs with aortic banding (n=6) exhibited significant left ventricular hypertrophy with increased stiffness compared with the control pigs (n=7) (end-diastolic pressure–volume relationship β: 0.053±0.017 versus 0.028±0.009 mm Hg/mL, *P*=0.007); however, all other parameters corresponding to systolic function, including ejection fraction, end-systolic pressure–volume relationship, preload recruitable stroke work, echocardiographic circumferential strain, and longitudinal strain, were not impaired in pigs with aortic banding. Relaxation parameters were also similar between groups. Sarcoplasmic reticulum calcium (Ca^{2+}) ATPase protein levels in the left ventricle were similar. There were significant increases in 3-dimensional echocardiographic left atrial volumes, suggesting the usefulness of these indexes to detect increased stiffness. Right atrial pacing with a heart rate of 120 beats per minute induced increased end-diastolic pressure in pigs with aortic banding in contrast to decreased end-diastolic pressure in the control pigs. Histological evaluation revealed that increased stiffness was accompanied by cardiomyocyte hypertrophy and increased perimysial and perivascular fibrosis.

***Conclusion*—**Increased stiffness is the major early pathological process that predisposes to congestive heart failure without abnormalities in systolic function and relaxation in a clinically relevant animal model of aortic stenosis. **(*J Am Heart Assoc*. 2015;4:e001925 doi: 10.1161/JAHA.115.001925)**

Key Words: diastolic dysfunction • fibrosis • hypertrophy • stiffness • systolic dysfunction

Transcatheter aortic valve implantation has emerged as an alternative therapeutic approach for patients with aortic stenosis. Implementation of this approach in clinical practice has expanded the population of candidates for aortic valve replacement, including patients with severe aortic stenosis who are considered high risk or ineligible for conventional surgical aortic valve replacement. These patients are often elderly with limited daily physical activity, and patients remain asymptomatic despite vulnerability to developing heart failure (HF); therefore, identifying the patient population with masked HF symptoms has become of increasing importance. To this end, it is essential to understand the underlying pathophysiology of HF development in severe aortic stenosis.

Newer techniques such as echocardiographic strain or magnetic resonance strain imaging allow for more detailed assessments of myocardial function than traditional modalities. Several studies have suggested the association of subnormal systolic function with HF in patients with severe aortic stenosis.[1–5] Meanwhile, others have reported impaired relaxation as a major contributor to HF development in aortic stenosis.[6,7] These changes, however, can be the result of disease progression and not the cause of HF. Consequently, it is not clear whether these abnormalities in systolic function

From the Cardiovascular Research Center, Icahn School of Medicine at Mount Sinai, New York, NY.

An accompanying Figure S1 is available at http://jaha.ahajournals.org/content/4/5/e001925/suppl/DC1

Correspondence to: Kiyotake Ishikawa, MD, Cardiovascular Research Center, Mount Sinai School of Medicine, One Gustave L. Levy Place, Box 1030, New York, NY 10029-6574. E-mail: kiyotake.ishikawa@mssm.edu

Received February 18, 2015; accepted April 8, 2015.

and relaxation are essential for HF development. We hypothesized that increased left ventricular (LV) stiffness is the major early abnormality in patients with severe aortic stenosis and that it predisposes these patients to congestive HF in the absence of systolic dysfunction or impaired relaxation. A large animal model that mimics human aortic stenosis was developed to test this hypothesis with comprehensive functional and histological assessments.

Methods

Animal Protocols

All animal protocols complied with the National Institutes of Health Guide for the Care and Use of Laboratory Animals and standards of US regulatory agencies. Protocols were approved by the institutional animal care and use committee of the Icahn School of Medicine at Mount Sinai. A total of 14 female Yorkshire pigs (Animal Biotech Industries (Danboro, PA)) were included in the study. Seven pigs received aortic banding (AoB) and were compared with control animals composed of 3 sham-operated animals and 4 naïve pigs of similar age at the final time point. Sham-surgery animals were included to provide an overview of changes in various parameters due to animal growth. The long-term animals underwent echocardiographic and hemodynamic assessments at 2 months after surgery, followed by final assessments at 3 to 5 months after surgery (Figure 1).

Yorkshire pigs were premedicated using intramuscular Telazol (8.0 mg/kg; Fort Dodge). After the placement of an intravenous line, animals were intubated and ventilated with 40% oxygen. General anesthesia was maintained with intravenous propofol (8 to 10 mg/kg per hour) throughout the procedure except for surgeries in which isoflurane (2% to 3%) was used. Intravenous saline infusion (body weight × 10 mL) was maintained for a period of 30 minutes under continuous monitoring to correct dehydration from overnight fasting. All animals then underwent echocardiographic assessment, followed by an AoB surgery at day 0 and hemodynamic measurements for other time points.

Aortic Banding

After an echocardiographic evaluation, pigs (10 to 13 kg) were positioned in the right lateral decubitus position, and left thoracotomy was performed in the third intercostal space. A 3-cm opening was created in the pericardium, and the ascending aorta proximal to the brachiocephalic artery was gently isolated. A 1-cm-thick customized rubber band with a fixed inner radius of 12 mm (approximate inner area of 4.5 cm^2) was placed around the aorta and fixed with umbilical tape. The chest was closed, air was evacuated, and animals recovered. Sham animals received pericardial opening without AoB.

Pressure and Volume Measurements

The methods for pressure measurement were previously described in detail.[8] Briefly, percutaneous punctures were performed to establish vascular access to the femoral artery

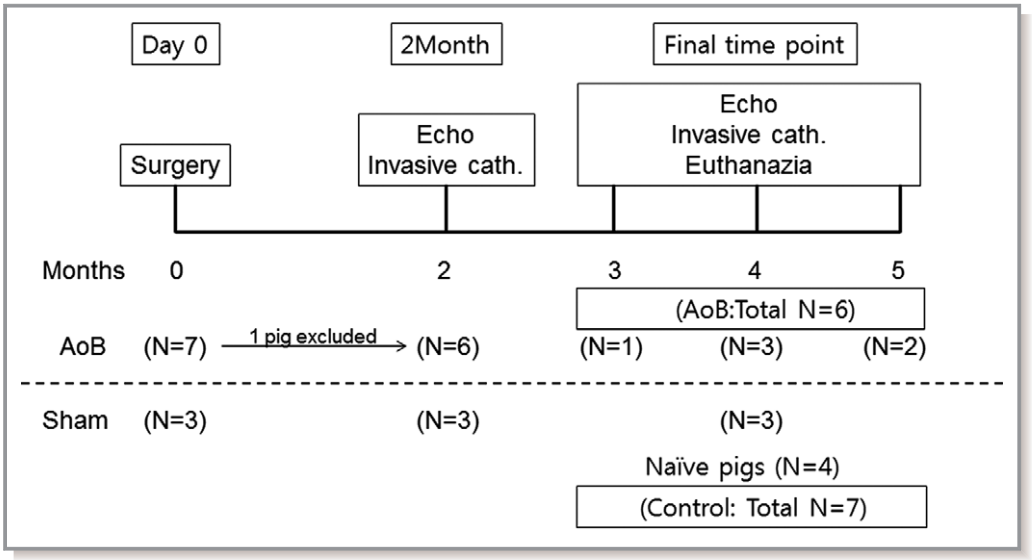

Figure 1. Study design and the number of animals. Two groups of animals were included in the study. Control group consists of 3 sham-surgery animals and 4 naïve pigs with similar age and weight to match the numbers of animals in the AoB group. One pig was euthanized at 1 month because of infectious aortic stenosis. AoB indicates aortic banding; cath., catheterization; Echo, echocardiography.

and femoral vein. Heparin (100 IU/kg intravenously) was administered to maintain an activated coagulation time of 150 to 250 seconds. A Swan-Ganz catheter (Edwards Lifesciences LLC) was advanced to the main pulmonary artery, and pressure measurements were collected. Next, through the femoral arterial sheath, a Millar catheter (Millar Instruments) was advanced to the left ventricle to obtain hemodynamic parameters. Approximately 0.25×body weight (in kilograms) milliliter of cold saline was injected into the inferior vena cava to obtain cardiac output by the thermodilution method. All measurements were performed after the confirmation of hemodynamic stability for 3 minutes. Data analyses were performed using an iox2 application (Emka Technologies). At the final time point, an inferior vena cava occlusion was conducted to evaluate the pressure–volume relationship during the preload reduction. The slope of the end-systolic pressure–volume relationship was defined as a measure of contractility. The stiffness constant (β) was determined from a set of relationships between end-diastolic pressure (EDP) and volume, using the following calculation: $EDP=\alpha e^{\beta \cdot EDV}$. EDV indicated end-diastolic volume, and α indicated the curve-fitting constant. After the preload-reduction study, a pacing catheter was advanced through the venous sheath. To evaluate the response of a physiologically relevant increase in heart rate, the right atrium was paced at 120 Hz, and hemodynamic parameters were measured again.

Echocardiographic Analysis

Comprehensive transthoracic echocardiographic studies including Doppler, 2-dimensional, and 3-dimensional (3D) echocardiograms were performed at baseline (prior to AoB), at 2 months after AoB, and at the final time point. A Philips iE-33 ultrasound system (Philips Medical Systems) was used to acquire echocardiographic data with a multifrequency imaging transducer (S5 probe for 2-dimensional images or X3 probe for 3D images). A subxiphoid approach provided an apical 4-chamber view and 3D images of the left ventricle. Using the parasternal approach, 3D images of the left atrium (Figure S1) and cross-sectional images of the LV short axis were obtained at the levels of the base, papillary muscle, and apex with a high frame rate (60 to 100 Hz). The 2-dimensional images were loaded into the Q-lab application (version 7.0; Philips Medical Systems) for strain analysis using a speckle-tracking algorithm. LV volumes and ejection fraction were obtained from 3D images. Body surface area (in square meters) was calculated as described previously,[9] and volume parameters were divided by body surface area to calculate volume indexes. Longitudinal strain was obtained from apical 4-chamber views. Short-axis images from the papillary muscle level were used for the circumferential strain analysis. Good inter- and intraobserver agreement was reported previously with this method.[10] Tissue Doppler images were analyzed to determine isovolumic relaxation time. Left atrium size was measured as the diameter from the right superior pulmonary vein to the root of the left appendage. The degree of stenosis due to AoB was serially evaluated by maximum velocity and the mean pressure gradient using the continuous-wave Doppler signal at each echocardiographic study by aligning the ultrasound beam with the aortic flow at the level of the banding in the apical view. In the absence of systolic dysfunction, these parameters are used as an established indicator of stenosis severity and allows classification of severe aortic stenosis when the mean gradient is >40 mm Hg, calculated by the simplified Bernoulli equation.[11]

Postmortem Molecular Analysis and Histology

At the end of the study protocol, the animals were euthanized by intravenous injection of potassium chloride under deep isoflurane anesthesia. Hearts were explanted and weighed, and the left ventricle was sectioned into 5 slices. One middle slice was used for histological and molecular analyses. Samples measuring 1 cm^3 were obtained from the anterior wall and preserved both by snap freezing and in formalin. Frozen cardiac tissue was minced and subsequently homogenized in radioimmunoprecipitation assay buffer containing a protease inhibitor cocktail (Sigma-Aldrich). Protein extracts (10 μg) were separated on 10% SDS-PAGE, transferred to a nitrocellulose membrane (Bio-Rad), and probed with antibodies specific for sarcoplasmic reticulum Ca^{2+} ATPase (SERCA2a; Cell Signaling) and phospholamban (Cell Signaling). Peroxidase-conjugated antibodies targeting both primary antibodies (Sigma-Aldrich) and GAPDH (Sigma-Aldrich) were also used. Blots were developed with SuperSignal West Pico (Pierce). Protein band densities were quantified using ImageJ software (National Institutes of Health). Formalin-fixed tissues were embedded in paraffin, sectioned (8 μm), and mounted on positively charged microscope slides. The slides were stained with fluorescein isothiocyanate–labeled wheat-germ agglutinin (Life Technologies) for assessing cell area as an indicator of hypertrophy and with picrosirus red (Abcam) to detect levels of collagen as an indicator of fibrosis.

Statistical Analysis

Data are expressed as mean±SD unless stated otherwise. The Shapiro–Wilk normality test was conducted to test the normality of the distribution. The unpaired *t* test was used to compare the differences between 2 groups, and the Mann–Whitney *U* test was used as appropriate. A paired *t* test was used to compare changes within the same animal. SPSS version 22.0 (IBM Corp) was used for all statistical analyses. A *P* value <0.05 was considered statistically significant.

Results

One pig in the AoB group was euthanized at 1 month after the surgery because of worsening general condition. Postmortem evaluation in this pig revealed infectious vegetation at the stenosis site. This pig was excluded from the analysis; therefore, the AoB group consisted of 6 pigs (Figure 1). There was no significant difference in the growth of the pigs, and most functional parameters remained nonsignificant at 2 months after the surgery, although this was most likely due to the small number of pigs in the sham group at this time point (Table 1). In the AoB group compared with the control group, echocardiographic assessments of pressure gradients (mean pressure gradient at

Table 1. Temporal Changes of Cardiac Parameters

	Baseline		2 Months			Final (3 to 5 Months)		
	AoB (n=6)	Sham (n=3)	AoB (n=6)	Sham (n=3)	*P* Value	AoB (n=6)	Control (n=7)	*P* Value
BW, kg	11.5±1.2	10.7±0.6	24.2±1.9	22.7±2.1	0.32	41.3±7.1	37.1±4.4	0.22
Days after surgery	0	0	57±3	55±1	0.53	121±20	107±8†	0.37
Echocardiography								
Ejection fraction (3DE), %	70.0±4.8	70.4±3.8	82.9±13.9	85.7±0.61	0.75	85.2±5.4	81.5±6.8	0.31
End-diastolic volume index (3DE), mL/m^2	72.1±16.9	78.3±15.7	69.4±20.3	81.7±7.1	0.35	81.9±11.7	87.1±10.3	0.41
End-systolic volume index (3DE), mL/m^2	21.6±6.1	22.9±2.9	11.2±7.7	11.7±1.3	0.92	11.8±3.7	15.6±4.7	0.14
Stroke volume index (3DE), mL/m^2	50.5±12.2	55.5±13.8	58.2±21.5	70.0±5.8	0.39	70.1±12.3	71.6±13.8	0.84
E wave, cm/s	62.5±11.6	72.3±19.1	65.8±13.5	61.1±3.7	0.58	61.4±14.1	71.1±7.0	0.14
E-wave deceleration time, ms	109±40	85±18	124±48	84±23	0.23	102±22	85±26	0.22
A wave, cm/s	52.6±8.1	60.7±12.9	66.6±8.4	56.5±12.6	0.19	74.4±13.5	70.0±14.5	0.58
E/A	1.20±0.27	1.18±0.07	1.02±0.36	1.12±0.30	0.68	0.82±0.07	1.05±0.22	0.03
E', cm/s	8.4±1.6	11.3±1.9	7.9±1.6	9.9±3.7	0.27	7.3±1.9	10.3±1.5	0.01
E/E'	7.5±1.0	6.3±0.6	8.5±1.6	6.9±2.9	0.31	8.7±2.3	7.0±1.1	0.10
IVRT, ms	71.8±26.3	71.1±8.3	76.8±14.9	70.3±6.0	0.39	95.1±25.8	80.4±8.2	0.23
LA diameter, mm	26.0±3.5	27.3±2.5	33.8±3.8	28.3±3.5	0.07	42.0±4.2	38.6±4.8	0.20
Left atrial ejection fraction (3DE), %	64.3±8.7	62.5±4.9	61.1±7.4	64.4±9.3	0.58	58.3±6.8	63.6±5.4	0.14
LA maximum volume index (3DE), mL/m^2	26.4±2.3	26.1±5.1	39.2±10.0	28.4±2.5	0.12	51 (34, 66)	29 (27, 43)	0.04*
LA minimum volume index (3DE), mL/m^2	9.4±2.7	9.7±1.5	15.3±5.5	10.0±2.3	0.16	23.1±12.9	12.1±2.7	0.05
Invasive hemodynamics								
LV maximum pressure, mm Hg	N/A	N/A	171±34	124±17	0.07	214 (186, 245)	132 (125, 141)	0.005*
End-diastolic pressure, mm Hg	N/A	N/A	20.1±4.0	13.8±4.4	0.07	16.7±4.8	14.4±3.4	0.34
Maximum dP/dt, mm Hg/s	N/A	N/A	2890±380	2055±350	0.02	2445±387	2331±528	0.67
dP/dt at pressure 40, mm Hg/s	N/A	N/A	1609±342	1641±226	0.89	1503±410	1644±310	0.5
Minimum dP/dt, mm Hg/s	N/A	N/A	−2100±592	−2277±445	0.67	−2870±1051	−2612±461	0.6
Tau, ms	N/A	N/A	52.9±11.4	59.7±8.4	0.39	47.2±16.7	53.1±8.8	0.46
Relaxation time, ms	N/A	N/A	119±14	140±13	0.06	118±12	131±17	0.13

Mean±SD. 3DE indicates 3-dimensional echocardiography; A, late diastolic transmitral flow velocity; AoB, aortic banding; BW, body weight; dP/dt, peak left ventricular pressure rate; E, early diastolic transmitral flow velocity; E', early diastolic mitral annular velocity; IVRT, isovolumic relaxation time; LA, left atrial; LV, left ventricular; N/A, not available.

*Mann–Whitney *U* test, median (interquartile range).

†Sham pigs.

2 months: 45.4±22.5 versus 1.7±1.2 mm Hg, P=0.01; final: 78.1±27.4 versus 3.7±2.1 mm Hg, P=0.003) and velocities (maximum velocity (V_{max}) at 2 months: 436±77 versus 93±23 cm/s, P<0.001; final: 510±130 versus 106±8 cm/s, P=0.001) at the banding sites increased significantly after surgery (Figure 2). There were nonsignificant increases in these parameters from 2 months to the final time point (V_{max} P=0.16, mean pressure gradient P=0.10), suggesting stenosis progression due to animal growth. At the final time point, pigs with AoB presented with significantly higher maximum LV pressure than control pigs. The hearts of the pigs with AoB exhibited significant hypertrophy, demonstrated by a higher ratio of heart weight to body weight (Figure 3).

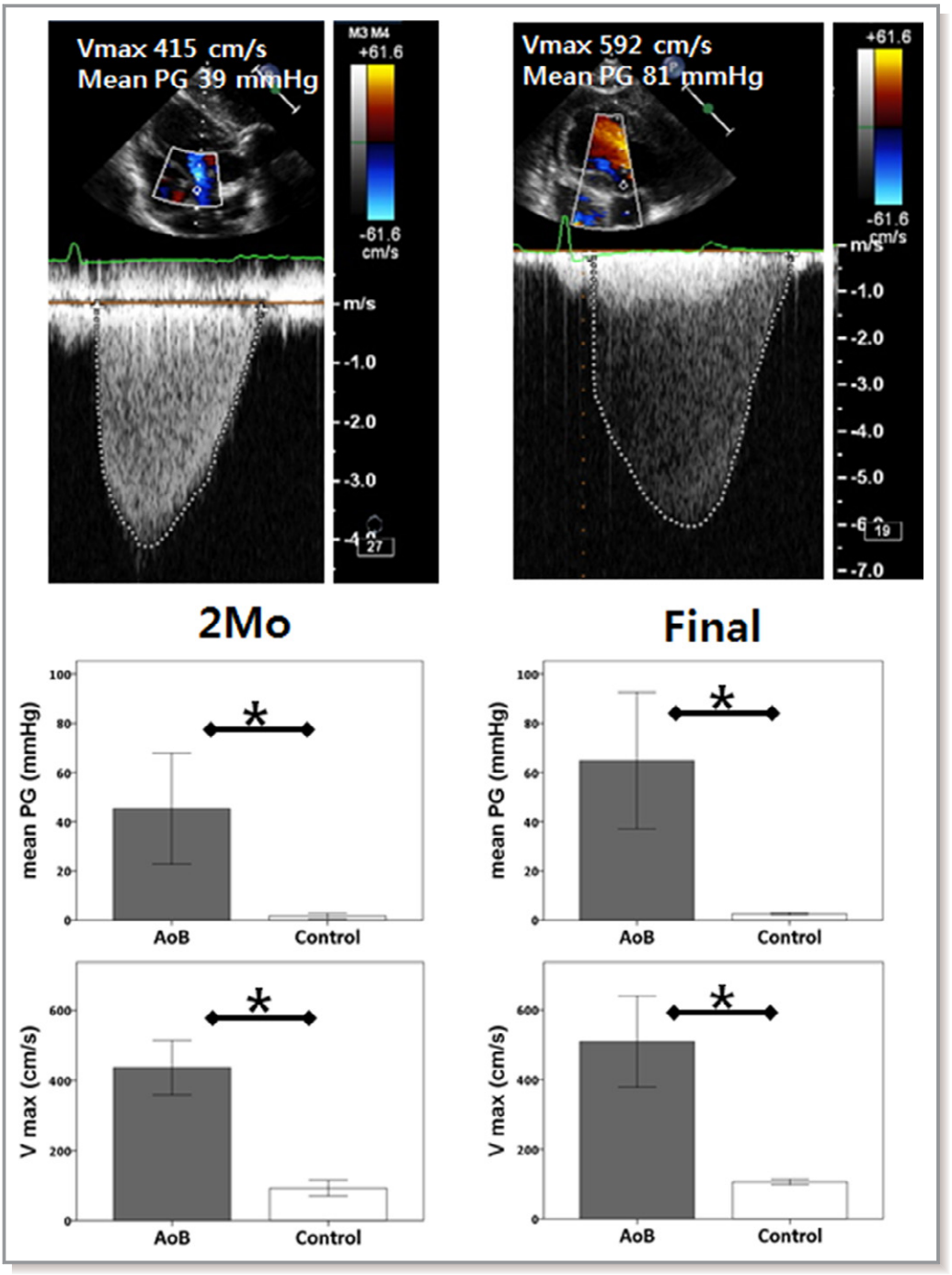

Figure 2. Echocardiographic assessment of stenosis at the aortic banding site using continuous Doppler. Both V_{max} and mean PG were significantly increased at 2 months and at final time points in AoB pigs. *P<0.05. AoB indicates aortic banding; PG, pressure gradient; V_{max}, maximum velocity.

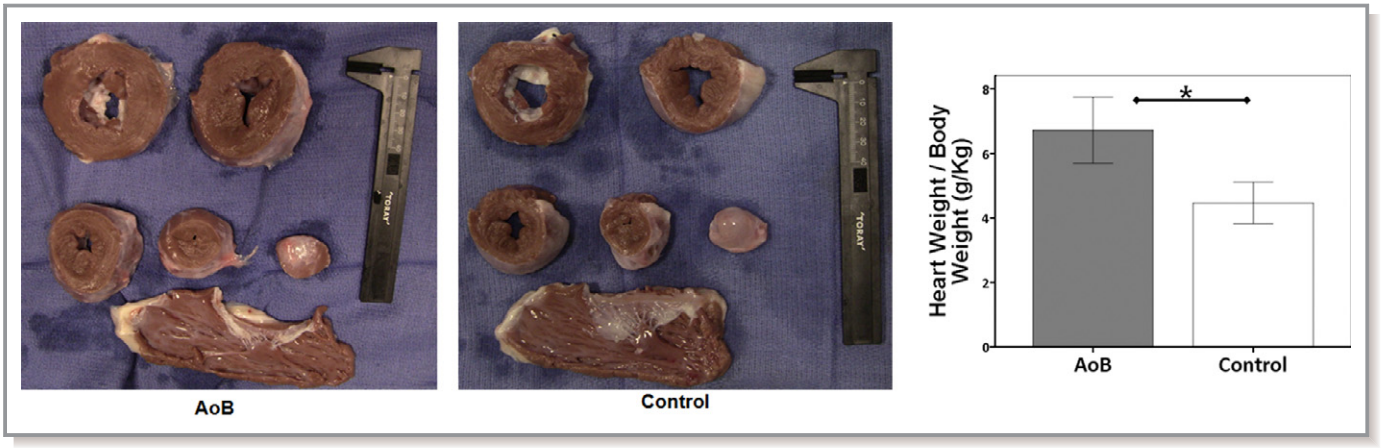

Figure 3. Cross-sections of the explanted heart. Macroscopic hypertrophy is apparent in pigs with aortic banding (AoB), with significantly heavier heart weight (P=0.001). *P<0.05.

Importantly, major systolic and relaxation parameters including LV ejection fraction by 3D echocardiography, peak LV pressure rate of rise, peak LV pressure rate of decline, Tau, and relaxation time were similar between the groups, indicating no depression in contractility and lusitropy in pigs with AoB (Table 1). These observations were supported by the pressure–volume analysis during the preload reduction study, in which higher end-systolic elastance and preload recruitable stroke work were demonstrated without impaired arterial–ventricular coupling (Figure 4, Table 2). Interestingly, LV EDP was not different between the groups, suggesting a compensating condition in pigs with AoB; however, pressure–volume relationship analysis revealed stiffer left ventricles in pigs with AoB, determined by significantly higher β of the end-diastolic pressure-volume relationship (Figure 4, Table 2).

Echocardiographic Strain and Left Atrial Volumes

Speckle-tracking strain analysis was performed at the final time point. All acquired images were adequate for strain analysis. Although pigs with AoB presented significant hypertrophy, there was no difference in longitudinal or circumferential strain between AoB and sham pigs (Figure 5). Left atrial 3D echocardiographic imaging exhibited significantly higher maximum and minimum left atrial volumes (Table 1).

Pacing Study

After baseline hemodynamic measurements were acquired, a pacing study was performed to examine the impact of increased heart rate within a physiological range. A pacing rate of 120 beats per minute in the right atrium increased LV EDP in pigs with AoB, whereas LV EDP decreased in the control animals (Figure 6). On average, there was an increase of ≈50% in EDP during pacing in pigs with AoB. These results indicate a propensity for developing congestive HF in these pigs. Changes in LV maximum pressure, LV pressure rate of rise and decline, and Tau were lower in pigs with AoB but did not reach statistical difference.

Postmortem Histology and SERCA2a Expression

Consistent with the macroscopic presentation, histological evaluation of the left ventricle confirmed cardiomyocyte hypertrophy in pigs with AoB (Figure 7). In addition, myocardium of pigs with AoB had significantly increased collagen volume fractions in both perimysial and perivascular areas (Figure 7). To investigate whether there was molecular evidence of systolic dysfunction, expression of SERCA2a and phospholamban was studied. We found no difference in these protein expression levels between the groups (Figure 8).

Discussion

In the present study, we demonstrated that increased LV stiffness alone, but not impaired LV systolic function or abnormal relaxation, is the major abnormality at the early stages of severe aortic stenosis in a clinically relevant experimental animal model; however, this increased LV stiffness was associated with a propensity to develop congestive HF in response to the physiological increase in heart rate despite the absence of systolic dysfunction and relaxation abnormalities. Normal systolic function was confirmed by comprehensive cardiac functional analyses including 3D echocardiography, pressure–volume relationship, and speckle-tracking echocardiographic strain. Consistent with our findings that relaxation and systolic function were normal, myocardial SERCA2a protein levels were similar between the groups. In contrast, LV stiffness evaluated by

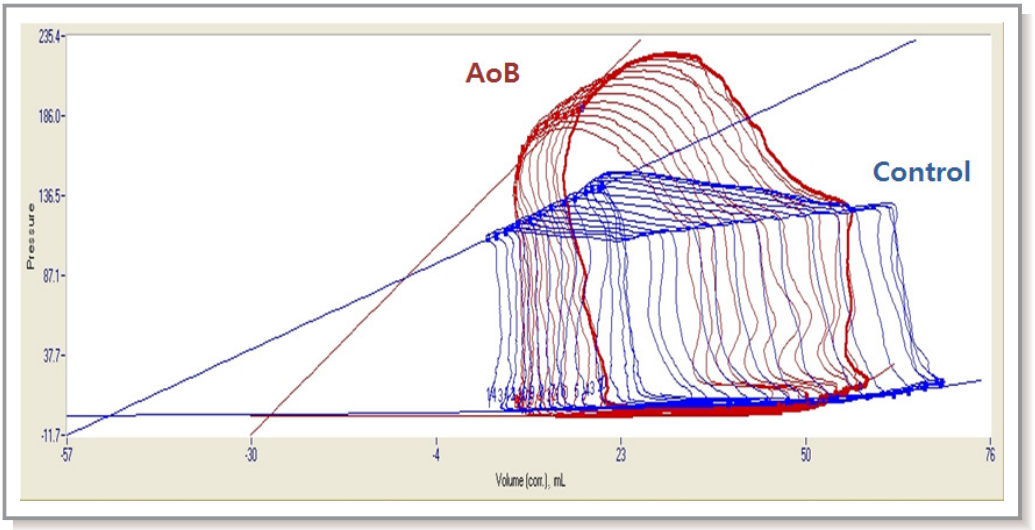

Figure 4. Representative pressure–volume loops of AoB and control pigs. Steeper end-systolic pressure–volume relationship was found in pigs with AoB compared with control pigs. Despite similar end-diastolic pressure before occlusion, pigs with AoB presented steeper end-diastolic pressure–volume relationship, indicating stiffer left ventricle. AoB indicates aortic banding; corr., corrected.

pressure–volume loop analysis revealed stiffer left ventricle in pigs after AoB. This finding is consistent with the severe myocardial hypertrophy observed in the pigs with AoB. Moreover, histopathological studies indicated that cardiomyocyte hypertrophy and increased fibrosis are major contributors to increased LV stiffness. To our knowledge, this study is the first to demonstrate isolated increased LV stiffness and its association with HF in the absence of systolic dysfunction and impaired relaxation in severe aortic stenosis, using comprehensive functional analyses.

Table 2. Pressure–Volume Loop Relationships

	AoB (N=6)	Control (n=7)	*P* Value
ESPVR			
Slope, mm Hg/mL	4.66 (2.83 to 5.74)	1.68 (1.13 to 1.90)	0.005*
V_0, mL	−29.8±22.0	−62.9±23.1	0.02
Ea/Ees	0.97±0.61	1.68±0.51	0.04
PRSW			
Slope, mm Hg	176 (103 to 202)	55 (48 to 81)	0.008*
EDPVR			
α	3.03±2.29	0.63±0.22	0.15
β	0.053±0.017	0.028±0.009	0.007

AoB indicates aortic banding; α, curve fitting constant; β, stiffness constant; Ea/Ees, arterial elastance/end-systolic elastance; EDPVR, end-diastolic pressure volume relationship; ESPVR, end-systolic pressure volume relationship; PRSW, preload recruitable stroke work; V_0, volume axis intercept of end-systolic pressure-volume relationship.
*Mann–Whitney *U* test, median (interquartile range).

Several large animal models of AoB have been developed previously, with use of dogs, pigs, and sheep showing varying results.[6,12–20] Although some studies have reported subnormal systolic function after AoB,[13,15,16] our animals did not develop systolic dysfunction up to 5 months after the surgery, with final LV maximum pressure >200 mm Hg. In contrast, our animals showed supranormal systolic function, as suggested by the increased slope of the end-systolic pressure–volume relationship, the higher preload recruitable stroke work, and the lower arterial–ventricular coupling. The discrepancy may be due to the time point examined after AoB, the age of the animals, and the degree of induced stenosis. The absence of systolic dysfunction with increased stiffness is an attractive feature of our model because it allows for isolation of LV stiffness and systolic dysfunction. This model also may be useful for evaluating various therapeutic approaches targeting HF with preserved ejection fraction; the presentation of this type of HF is similar, with increased myocardial stiffness as a major contributor to development of HF in both diseases.

Relaxation and stiffness are sometimes discussed together as a form of diastolic dysfunction without clear distinction. This is because in many cases, impaired relaxation and increased stiffness coexist in diastolic dysfunction; however, our pigs with AoB presented with increased stiffness without delayed relaxation. Consistent with this finding, it was reported that a mouse model of α-myosin heavy chain missense mutation presented significantly impaired relaxation in the absence of HF or elevated EDP.[21,22] These data suggest that relaxation and stiffness abnormalities do not necessarily parallel and that increased stiffness alone is the key factor for

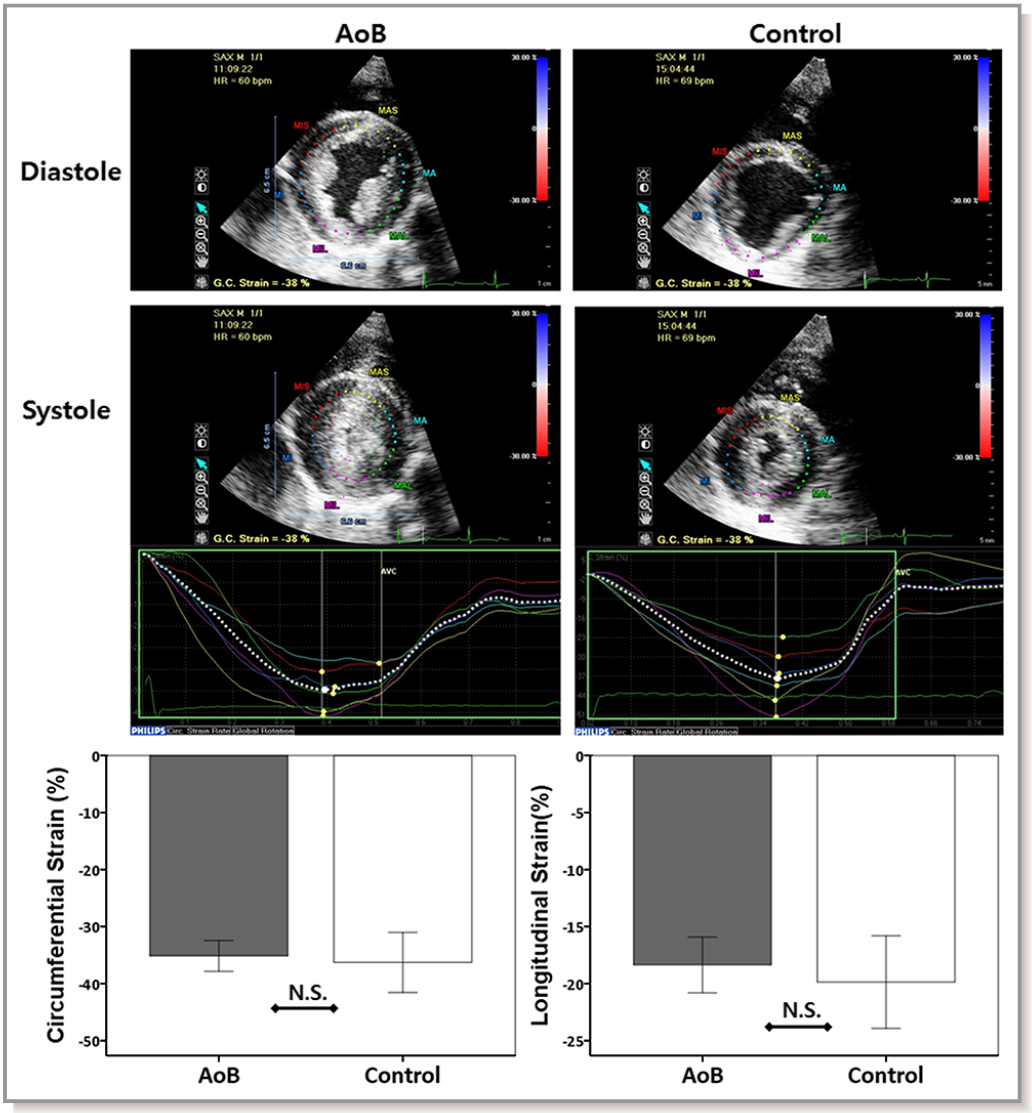

Figure 5. Echocardiographic speckle-tracking strain analysis. AoB pigs exhibited thicker wall thickness at both end-diastole and end-systole (top); however, both peak circumferential and longitudinal strains were not different between the groups (P=0.63 and P=0.45, respectively) (bottom). AoB indicates aortic banding; bpm, beats per minute; GC, global circumferential, HR, heart rate; NS, not significant.

HF induction. They also highlight the importance of distinguishing relaxation and stiffness when evaluating HF with diastolic abnormalities. We found that increased cardiomyocyte hypertrophy and increased fibrosis were potential contributors to increased LV stiffness. A recent study in a rat model of swimming-induced cardiac hypertrophy without significant myocardial fibrosis reported improved LV relaxation without altered stiffness.[23] Although it remains speculative, fibrosis seems to have a significant impact on LV stiffness, although the amount is minor in our model.

Our findings have important clinical implications. If subnormal systolic function or impaired LV relaxation is the key early indicator of HF development in patients with severe aortic stenosis, clinicians can focus on detailed functional imaging studies to identify these abnormalities. Unfortunately, our study demonstrated that this is not the case, and thus patients with severe aortic stenosis are at risk of developing congestive HF without any evidence of systolic dysfunction or impaired relaxation. Instead, increased LV stiffness seems to be the critical early pathological process that predisposes to congestive HF development in this model. Precise measurement of LV stiffness requires pressure–volume loop analysis using invasive catheterization and load-alteration studies. Several formulas for estimating LV stiffness have been proposed,[24,25] but these formulas contain many assumptions, and whether they are always applicable to different disease conditions remains unclear. Consequently, identifying the early manifestation of HF in asymptomatic severe aortic

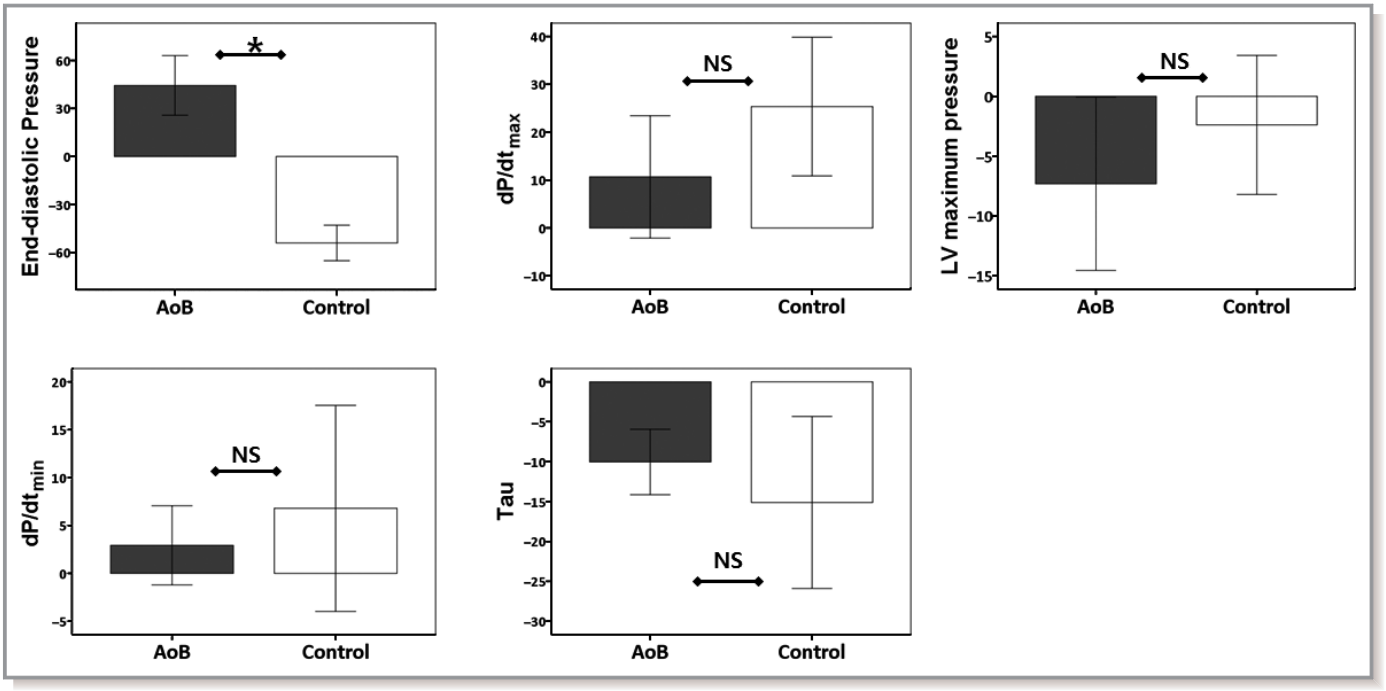

Figure 6. Hemodynamic changes induced by pacing study. Pigs received right atrial pacing (120 bpm) with continuous hemodynamic monitoring. End-diastolic pressure decreased in the control group but increased in the AoB group ($P<0.001$), suggesting the propensity of the latter to develop congestive heart failure. Although the parameters did not reach statistical significance, changes in dP/dt_{max}, dP/dt_{min}, and Tau were smaller in AoB pigs, suggesting limited functional reserve. *$P<0.05$. AoB indicates aortic banding; bpm, beats per minute; dP/dt_{max}, peak left ventricular pressure rate of rise; dP/dt_{min}, peak left ventricular pressure rate of decline; LV, left ventricular; NS, not significant.

stenosis patients remains challenging. Although most studies of patients with severe aortic stenosis report the presence of diastolic functional abnormalities,[26,27] comprehensive evaluation of specific diastolic parameters is not yet available using standard noninvasive tools; therefore, in current guidelines, diastolic functional parameters are not included in the decision-making process for patients with severe aortic stenosis.[28] Our results demonstrated that 3D echocardiography–derived left atrial volumes were significantly increased in pigs after AoB, and these indexes had superior sensitivity relative to conventional 2-dimensional left atrial diameter to detect the difference between groups. The left atrium is constantly exposed to increased LV filling pressure in a stiff heart, promoting left atrial remodeling. In fact, left atrial remodeling has been proposed as a chronic marker for diastolic dysfunction.[29] Focused evaluation of the left atrium using sophisticated techniques may provide better diagnostic information in patients with severe aortic stenosis. Another approach that may be useful in the detection of early signs of HF in this patient population is fibrosis evaluation, based on our findings. Noninvasive quantification of fibrosis may be performed with serum markers[30] or with cardiac magnetic resonance. In fact, several studies have shown correlation between fibrosis assessed by histology and cardiac magnetic resonance imaging using late gadolinium enhancement[31,32] and T1 mapping[33] in patients with severe aortic stenosis. Because these correlations were evaluated in patients with a relatively large degree of fibrosis, further study is necessary to examine cardiac magnetic resonance sensitivity to small increases in myocardial fibrosis, as found in our study. From a therapeutic point of view, our findings suggest that antihypertrophic and antifibrotic therapies may be beneficial to prevent the development of HF in patients with aortic stenosis.

Limitations

Due to the nature of animal studies, whether the pigs had HF symptoms remains uncertain, although we did not find any difference in the pig behaviors compared with the sham animals. The propensity for development of congestive HF was determined by increased EDP during the pacing study. Ideally, this should be performed by exercise testing; however, the difficulty of training the pigs for adequate exercise testing and of performing stable placement of the pressure–volume catheter during exercise precluded this option. The pacing method to mimic exercise has been reported previously,[14] and the clear difference in response to pacing in our study suggests the utility of this method to uncover the propensity for HF development in patients with limited exercise ability.

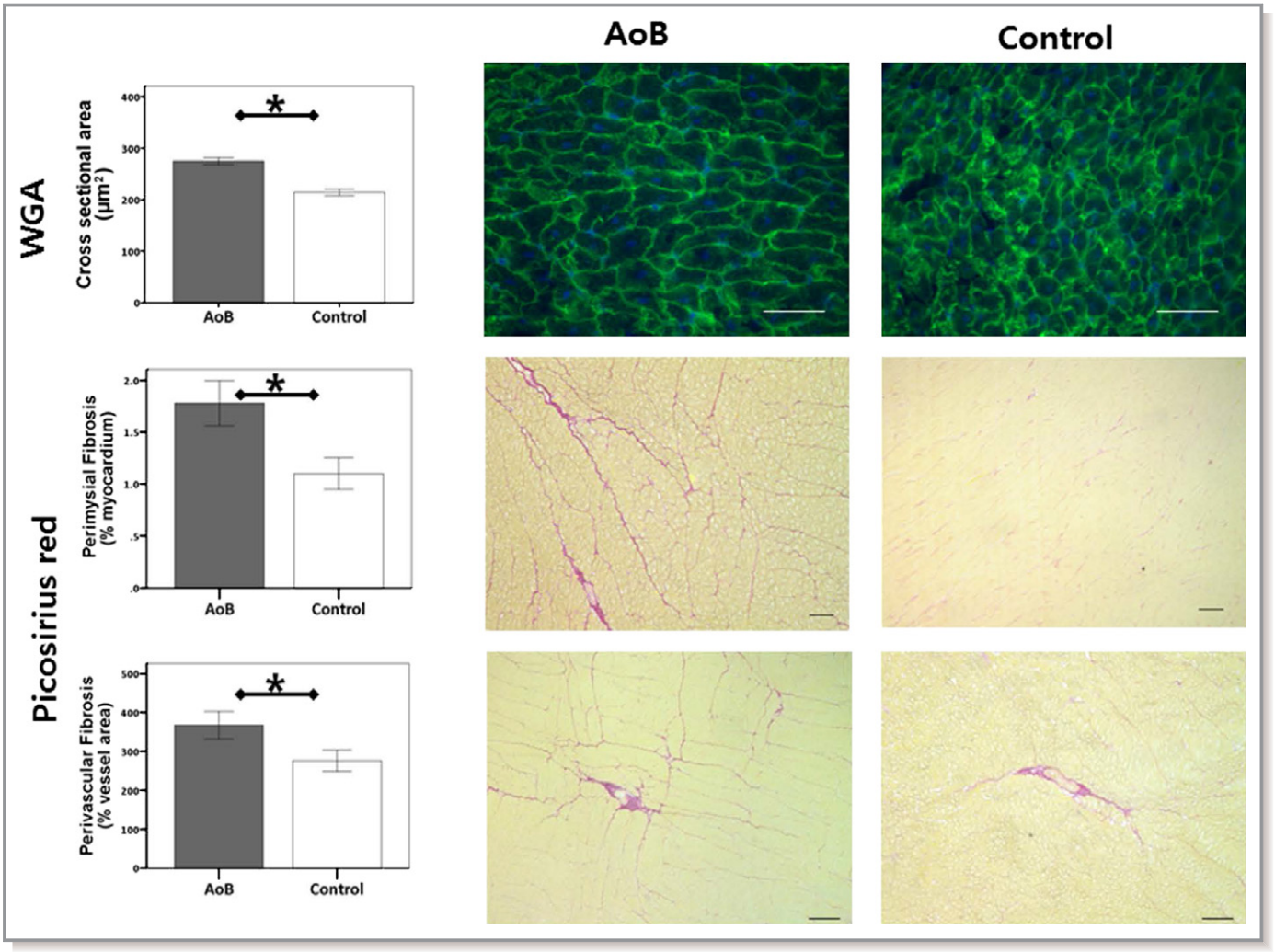

Figure 7. Histological characterization of the left ventricular myocardium. AoB pigs presented a significantly larger cardiomyocyte area ($P<0.001$), increased perimysial fibrosis ($P=0.01$), and increased perivascular fibrosis ($P=0.045$). Scale bars indicate 50 μm for WGA figures, 200 μm for perimysial fibrosis figures, and 100 μm for perivascular fibrosis figures. Error bars indicate standard error. *$P<0.05$. AoB indicates aortic banding; WGA, wheat-germ agglutinin.

The supracoronary stenosis in the AoB pig model may differ in the coronary flow pattern from valvular stenosis in humans; however, impaired coronary flow similar to human aortic stenosis has been shown in a dog model of AoB with a banding location similar to ours.[14] Not all animals in the control group underwent sham surgery, and this may have caused unrecognized heterogeneity in this group related to the surgical procedures.

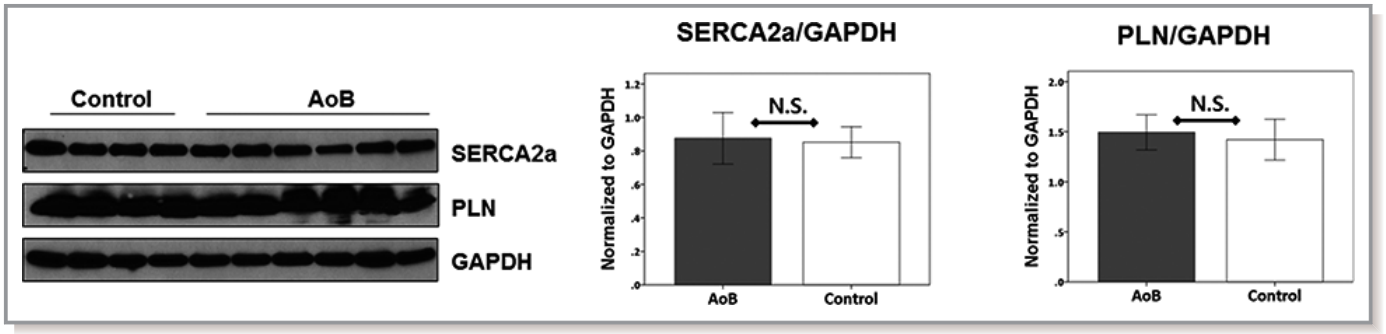

Figure 8. SERCA2a and PLN expression in the left ventricle. Both SERCA2a and PLN levels were not different between the AoB and control groups. AoB indicates aortic banding; NS, not significant; PLN, phospholamban; SERCA2a, sarcoplasmic reticulum calcium ($Ca2^{+}$) ATPase.

Conclusion

Early abnormality in severe aortic stenosis is characterized by increased LV stiffness, whereas systolic dysfunction or impaired relaxation is not necessarily present in this early pathological process. Increased LV stiffness due to cardiomyocyte hypertrophy and increased tissue fibrosis contributes to the propensity to develop congestive HF. Our animal model offers a unique opportunity to study the role of LV stiffness independent of systolic dysfunction and impaired relaxation.

Sources of Funding

This work is supported by National Institutes of Health R01 HL117505, HL 119046, a National Heart, Lung, and Blood Institute (NHLBI) Program of Gene Therapy Resource Program (GTRP), and Excellence in Nanotechnology (PEN) Award, Contract No. HHSN268201000045C, a P50HL112324, and a Transatlantic Fondation Leducq Grant. Aguero was supported by Spanish Society of Cardiology (Ischemic Heart Disease section) and Fundacion Alfonso Martin-Escudero. NH was supported by a grant from the French Federation of Cardiology.

Disclosures

None.

Reference

1. Poulsen SH, Sogaard P, Nielsen-Kudsk JE, Egeblad H. Recovery of left ventricular systolic longitudinal strain after valve replacement in aortic stenosis and relation to natriuretic peptides. *J Am Soc Echocardiogr*. 2007;20:877–884.
2. Dinh W, Nickl W, Smettan J, Kramer F, Krahn T, Scheffold T, Barroso MC, Brinkmann H, Koehler T, Lankisch M, Futh R. Reduced global longitudinal strain in association to increased left ventricular mass in patients with aortic valve stenosis and normal ejection fraction: a hybrid study combining echocardiography and magnetic resonance imaging. *Cardiovasc Ultrasound*. 2010;8:29.
3. Yingchoncharoen T, Gibby C, Rodriguez LL, Grimm RA, Marwick TH. Association of myocardial deformation with outcome in asymptomatic aortic stenosis with normal ejection fraction. *Circ Cardiovasc Imaging*. 2012;5:719–725.
4. Ng AC, Delgado V, Bertini M, Antoni ML, van Bommel RJ, van Rijnsoever EP, van der Kley F, Ewe SH, Witkowski T, Auger D, Nucifora G, Schuijf JD, Poldermans D, Leung DY, Schalij MJ, Bax JJ. Alterations in multidirectional myocardial functions in patients with aortic stenosis and preserved ejection fraction: a two-dimensional speckle tracking analysis. *Eur Heart J*. 2011;32:1542–1550.
5. Lafitte S, Perlant M, Reant P, Serri K, Douard H, DeMaria A, Roudaut R. Impact of impaired myocardial deformations on exercise tolerance and prognosis in patients with asymptomatic aortic stenosis. *Eur J Echocardiogr*. 2009;10:414–419.
6. Marshall KD, Muller BN, Krenz M, Hanft LM, McDonald KS, Dellsperger KC, Emter CA. Heart failure with preserved ejection fraction: chronic low-intensity interval exercise training preserves myocardial O_2 balance and diastolic function. *J Appl Physiol*. 2013;114:131–147.
7. Falcao-Pires I, Palladini G, Goncalves N, van der Velden J, Moreira-Goncalves D, Miranda-Silva D, Salinaro F, Paulus WJ, Niessen HW, Perlini S, Leite-Moreira AF. Distinct mechanisms for diastolic dysfunction in diabetes mellitus and chronic pressure-overload. *Basic Res Cardiol*. 2011;106:801–814.
8. Ishikawa K, Chemaly ER, Tilemann L, Fish K, Ladage D, Aguero J, Vahl T, Santos-Gallego C, Kawase Y, Hajjar RJ. Assessing left ventricular systolic dysfunction after myocardial infarction: are ejection fraction and dP/dt(max) complementary or redundant? *Am J Physiol Heart Circ Physiol*. 2012;302:H1423–H1428.
9. Kelley KW, Curtis SE, Marzan GT, Karara HM, Anderson CR. Body surface area of female swine. *J Anim Sci*. 1973;36:927–930.
10. Ishikawa K, Kawase Y, Ladage D, Chemaly ER, Tilemann L, Fish K, Sanz J, Garcia MJ, Hajjar RJ. Temporal changes of strain parameters in the progress of chronic ischemia: with comparison to transmural infarction. *Int J Cardiovasc Imaging*. 2012;28:1671–1681.
11. Baumgartner H, Hung J, Bermejo J, Chambers JB, Evangelista A, Griffin BP, Iung B, Otto CM, Pellikka PA, Quinones M. Echocardiographic assessment of valve stenosis: EAE/ASE recommendations for clinical practice. *J Am Soc Echocardiogr*. 2009;22:1–23.
12. Ghaleb B, Hittinger L, Kim SJ, Kudej RK, Iwase M, Uechi M, Berdeaux A, Bishop SP, Vatner SF. Selective large coronary endothelial dysfunction in conscious dogs with chronic coronary pressure overload. *Am J Physiol*. 1998;274:H539–H551.
13. Tagawa H, Koide M, Sato H, Zile MR, Carabello BA, Cooper G IV. Cytoskeletal role in the transition from compensated to decompensated hypertrophy during adult canine left ventricular pressure overloading. *Circ Res*. 1998;82:751–761.
14. Nakano K, Corin WJ, Spann JF Jr, Biederman RW, Denslow S, Carabello BA. Abnormal subendocardial blood flow in pressure overload hypertrophy is associated with pacing-induced subendocardial dysfunction. *Circ Res*. 1989;65:1555–1564.
15. Moorjani N, Catarino P, Trabzuni D, Saleh S, Moorji A, Dzimiri N, Al-Mohanna F, Westaby S, Ahmad M. Upregulation of Bcl-2 proteins during the transition to pressure overload-induced heart failure. *Int J Cardiol*. 2007;116:27–33.
16. Koide M, Nagatsu M, Zile MR, Hamawaki M, Swindle MM, Keech G, DeFreyte G, Tagawa H, Cooper G IV, Carabello BA. Premorbid determinants of left ventricular dysfunction in a novel model of gradually induced pressure overload in the adult canine. *Circulation*. 1997;95:1601–1610.
17. Nediani C, Formigli L, Perna AM, Ibba-Manneschi L, Zecchi-Orlandini S, Fiorillo C, Ponziani V, Cecchi C, Liguori P, Fratini G, Nassi P. Early changes induced in the left ventricle by pressure overload. An experimental study on swine heart. *J Mol Cell Cardiol*. 2000;32:131–142.
18. Wisenbaugh T, Allen P, Cooper G IV, Holzgrefe H, Beller G, Carabello B. Contractile function, myosin ATPase activity and isozymes in the hypertrophied pig left ventricle after a chronic progressive pressure overload. *Circ Res*. 1983;53:332–341.
19. Yarbrough WM, Mukherjee R, Stroud RE, Rivers WT, Oelsen JM, Dixon JA, Eckhouse SR, Ikonomidis JS, Zile MR, Spinale FG. Progressive induction of left ventricular pressure overload in a large animal model elicits myocardial remodeling and a unique matrix signature. *J Thorac Cardiovasc Surg*. 2012;143:215–223.
20. Ye Y, Gong G, Ochiai K, Liu J, Zhang J. High-energy phosphate metabolism and creatine kinase in failing hearts: a new porcine model. *Circulation*. 2001;103:1570–1576.
21. Georgakopoulos D, Christe ME, Giewat M, Seidman CM, Seidman JG, Kass DA. The pathogenesis of familial hypertrophic cardiomyopathy: early and evolving effects from an alpha-cardiac myosin heavy chain missense mutation. *Nat Med*. 1999;5:327–330.
22. Geisterfer-Lowrance AA, Christe M, Conner DA, Ingwall JS, Schoen FJ, Seidman CE, Seidman JG. A mouse model of familial hypertrophic cardiomyopathy. *Science*. 1996;272:731–734.
23. Radovits T, Olah A, Lux A, Nemeth BT, Hidi L, Birtalan E, Kellermayer D, Matyas C, Szabo G, Merkely B. Rat model of exercise-induced cardiac hypertrophy: hemodynamic characterization using left ventricular pressure-volume analysis. *Am J Physiol Heart Circ Physiol*. 2013;305:H124–H134.
24. Zile MR, Baicu CF, Gaasch WH. Diastolic heart failure–abnormalities in active relaxation and passive stiffness of the left ventricle. *N Engl J Med*. 2004;350:1953–1959.
25. Marino P, Little WC, Rossi A, Barbieri E, Anselmi M, Destro G, Prioli A, Lanzoni L, Zardini P. Can left ventricular diastolic stiffness be measured noninvasively? *J Am Soc Echocardiogr*. 2002;15:935–943.
26. Otto CM, Burwash IG, Legget ME, Munt BI, Fujioka M, Healy NL, Kraft CD, Miyake-Hull CY, Schwaegler RG. Prospective study of asymptomatic valvular aortic stenosis. Clinical, echocardiographic, and exercise predictors of outcome. *Circulation*. 1997;95:2262–2270.
27. Hachicha Z, Dumesnil JG, Pibarot P. Usefulness of the valvuloarterial impedance to predict adverse outcome in asymptomatic aortic stenosis. *J Am Coll Cardiol*. 2009;54:1003–1011.
28. Nishimura RA, Otto CM, Bonow RO, Carabello BA, Erwin JP III, Guyton RA, O'Gara PT, Ruiz CE, Skubas NJ, Sorajja P, Sundt TM III, Thomas JD, Members

AATF. 2014 AHA/ACC guideline for the management of patients with valvular heart disease: executive summary: a report of the American College of Cardiology/American Heart Association Task Force on Practice Guidelines. *Circulation*. 2014;129:2440–2492.

29. Abhayaratna WP, Seward JB, Appleton CP, Douglas PS, Oh JK, Tajik AJ, Tsang TS. Left atrial size: physiologic determinants and clinical applications. *J Am Coll Cardiol*. 2006;47:2357–2363.

30. Jellis C, Martin J, Narula J, Marwick TH. Assessment of nonischemic myocardial fibrosis. *J Am Coll Cardiol*. 2010;56:89–97.

31. Azevedo CF, Nigri M, Higuchi ML, Pomerantzeff PM, Spina GS, Sampaio RO, Tarasoutchi F, Grinberg M, Rochitte CE. Prognostic significance of myocardial fibrosis quantification by histopathology and magnetic resonance imaging in patients with severe aortic valve disease. *J Am Coll Cardiol*. 2010;56:278–287.

32. Weidemann F, Herrmann S, Stork S, Niemann M, Frantz S, Lange V, Beer M, Gattenlohner S, Voelker W, Ertl G, Strotmann JM. Impact of myocardial fibrosis in patients with symptomatic severe aortic stenosis. *Circulation*. 2009;120:577–584.

33. White SK, Sado DM, Fontana M, Banypersad SM, Maestrini V, Flett AS, Piechnik SK, Robson MD, Hausenloy DJ, Sheikh AM, Hawkins PN, Moon JC. T1 mapping for myocardial extracellular volume measurement by CMR: bolus only versus primed infusion technique. *JACC Cardiovasc Imaging*. 2013;6:955–962.